Springer

Journal of
Mechanical
Science and
Technology

Journal of Mechanical Science and Technology 22 (2008) 1747~1756

www.springerlink.com/content/1738-494x
DOI 10.1007/s12206-008-0517-3

Effect of manufacturing tolerances on dynamic equilibria of multibody systems undergoing prescribed rotational motion

Dong Hwan Choi[1,*], Jonathan A. Wickert[1] and Hong Hee Yoo[2]

[1]*Department of Mechanical Engineering Iowa State University Ames, IA 50011 USA*
[2]*Department of Mechanical Engineering Hanyang University Seoul 133-791 Korea, Republic of*

(Manuscript Received February 25, 2008; Revised May 9, 2008; Accepted May 17, 2008)

Abstract

A general formulation is developed for the tolerance analysis of dynamic equilibria in a multibody system undergoing prescribed rotational motion, with applications including robots, spacecraft, propulsion and power generation systems, and sensors and actuators. In a state of dynamic equilibrium, a subset of the generalized coordinates assumes constant values while the remaining coordinates vary and respond in time. Manufacturing tolerances can be mathematically represented by probabilistic distributions or statistical variables through either an analytical approach or a Monte Carlo simulation. In the present tolerance work, the tolerances of design parameters including lengths, stiffnesses, inertias, and attachment positions are examined. In order to analytically calculate the statistical response of the dynamic equilibrium positions to such tolerances, the first-order sensitivities of the equilibria with respect to parameters are calculated. To illustrate the method's accuracy and computational efficiency, two numerical examples are considered, and the statistical results obtained analytically for the equilibria are compared with those calculated through Monte Carlo simulation. In some cases, an equilibrium configuration can have an operating condition for which the response has zero standard deviation to perturbations of a design parameter. That condition can be a useful design point to the extent that typical manufacturing tolerances or other sources of variation would have no effect on the dynamic equilibrium configuration.

Keywords: Dynamic equilibria; Manufacturing tolerance; Multibody systems; Monte Carlo simulation; Zero standard deviation

1. Introduction

In a dynamic equilibrium state, a subset of generalized coordinates assumes constant values while the remaining coordinates vary and evolve in time. Such equilibria can develop in multibody systems that undergo prescribed rotational motions, as is the case in some applications including robotics, deploying spacecraft appendages, propulsion and power generation, and microelectromechanical sensors and actuators. Examples of open loop systems that exhibit dynamic equilibria have been discussed [1-3] in the context of Newton, Lagrange, and Kane methods. However, dynamic equilibria often cannot be calculated efficiently through existing commercial codes [4-6] to the extent that they do not capture the appropriate physics of the system at hand. In one approach to a constrained multibody system's dynamic equilibrium configuration, the transient response of certain coordinates can be simulated for prescribed input motion until the coordinates reach steady state at the values associated with the equilibrium. However, the computational effort associated with that time integration procedure, with the goal of only identifying an equilibrium state, can be costly and prohibitive.

Choi *et al.* [7] described a general formulation to calculate directly the coordinate values in a dynamic equilibrium state for a constrained multibody system having prescribed rotational motion. In that case, relative coordinates [8] and a velocity transformation

*Corresponding author. Tel.: +1 515 294 6776, Fax.: +1 515 294 3261
E-mail address: dhchoi@iastate.edu

technique [9] were used to obtain the equations of motion and identify the equilibrium values of the coordinates.

However, in the field, unwanted dynamic equilibrium positions of a mechanical system having prescribed rotational motions can arise from the uncontrolled imposed angular velocity or the manufacturing tolerances that are associated with design variables. Those manufacturing tolerance errors are preferentially maintained within a certain range in order for the system to achieve satisfactory performance. Although the response error can be improved by tightening the component and manufacturing tolerances, such a remedy is often costly. The constraints of manufacturing expense and response errors frame a mechanical design optimization problem.

The mechanical error in a mechanism or a linkage system originates primarily from clearances within its joints, and a rich literature describes the effects of joint clearance and contact modeling issues for mechanical systems. The pioneering work of Hartenberg and Denavit [10] addressed the issue of mechanical errors in linkage systems, and they estimated the magnitude of mechanical errors based on the maximum allowable tolerances for the link lengths. In essence, that deterministic approach focused on the worst case combination of the tolerances present. Garrett and Hall [11] developed a statistical means to calculate the mechanical errors arising from joint clearance tolerances; they represented the errors in terms of mobility bands calculated through Monte Carlo simulation of a four-bar linkage system. Dubowsky and Freudenstein [12] introduced the concept of an impact pair for the joints in a linkage. Recently, with application to continuous contact modeling issues in multibody systems, Ravn [13] suggested a continuous analysis approach for planar multibody systems in terms of a multibody dynamics formulation and Hertzian contact. Flores et al. [14] presented a method to deal with the influence of the spherical clearance joints in spatial multibody systems by using a continuous contact force model.

With respect to a statistical view of joint clearance problem, Lee [15] presented an analytical model for effective link length that is based upon a first-order Taylor series expansion. Lee and Gilmore [16] subsequently generalized that method to incorporate the uncertainties associated with pin locations and variations in link length. With a generalized vector loop-based model to represent small kinematic adjustments, Chase et al. [17] presented the direct linearization method (DLM) for the tolerance analysis of two-dimensional mechanisms. Choi et al. [18] present a computational algorithm for the dynamic analysis of multibody systems considering both probabilistic and statistical properties. The literature associated with the effects of joint clearance has primarily emphasized behavior and contact modeling issues, as well as dynamic and kinematic responses.

It is an objective of this study to present an algorithm which deals with the effects of tolerances in various design parameters upon the dynamic equilibria of spatial multibody systems undergoing a prescribed rotational motion. A general multibody formulation, relative coordinates [8], and a velocity transformation technique [9] are used to obtain the equations of motion and to identify the dynamic equilibria. The tolerance analysis is based on a statistical approach [18] and a Monte Carlo simulation.

In order to analytically calculate the statistical results of the dynamic equilibrium positions, the first-order sensitivities of the dynamic equilibria with respect to a design parameter are required. Therefore, an efficient computational algorithm based upon direct differentiation is newly developed to calculate the first-order sensitivities with respect to the design parameter. To verify the method's effectiveness, two numerical examples are described: an open loop system and a closed loop system. The statistical results obtained analytically are compared with those obtained by Monte Carlo simulations, and the relative advantages and disadvantages of two methods are outlined.

2. Tolerance analysis

The general response of a complex spatial mechanism having a multiplicity of design variables, such as a spring's stiffness, inertia, a joint's attachment position, and link lengths, is determined through a multibody dynamics formulation [19]. The response metrics include positions, velocities, accelerations, and forces throughout the system. Generally, explicit mathematical relationships between the design variables and the response metrics are not available, but the influence of the tolerances on the statistical properties of those metrics can be obtained through the procedure outlined in what follows.

The response variable $\mathbf{Y}$, if not known explicitly, can be expressed symbolically through simulation as

the function

$$\mathbf{Y} = \mathbf{Y}(b_1, b_2, \ldots, b_n) \tag{1}$$

of independent design variables b_i. By expanding $\mathbf{Y}(b_1, b_2, \ldots, b_n)$ about the mean values $\bar{b}_i$,

$$\mathbf{Y} = \mathbf{Y}(\bar{b}_1, \bar{b}_2, \ldots, \bar{b}_n) + \sum_{i=1}^{n}(b_i - \bar{b}_i)\frac{\partial \mathbf{Y}}{\partial b_i} + \frac{1}{2}\sum_{i=1}^{n}\sum_{j=1}^{n}(b_i - \bar{b}_i)(b_j - \bar{b}_j)\frac{\partial^2 \mathbf{Y}}{\partial b_i \partial b_j} + \ldots \tag{2}$$

If the means and variances of the b_i are known, the mean and the variance of $\mathbf{Y}$ can likewise be estimated by a Taylor series expansion. The first-order mean of $\mathbf{Y}$, denoted $\bar{\mathbf{Y}}$, becomes

$$\bar{\mathbf{Y}} = \mathbf{Y}(\bar{b}_1, \bar{b}_2, \ldots, \bar{b}_n) \tag{3}$$

and can be approximated in terms of $\bar{b}_i$. The first-order variance of $\mathbf{Y}$, denoted $Var(\mathbf{Y})$, likewise becomes

$$Var(\mathbf{Y}) = \left(\boldsymbol{\sigma}^{\mathbf{Y}}\right)^2 = \sum_{i=1}^{n}\left(\frac{\partial \mathbf{Y}}{\partial b_i}\right)^2 Var(b_i) + \frac{1}{2}\sum_{i=1}^{n}\sum_{j=1}^{n}\frac{\partial \mathbf{Y}}{\partial b_i}\frac{\partial \mathbf{Y}}{\partial b_j}Cov(b_i, b_j) \quad i \neq j \tag{4}$$

where $\boldsymbol{\sigma}^{\mathbf{Y}}$ denotes the standard deviation of $\mathbf{Y}$ and $Cov(b_i, b_j)$ denotes the covariance of the two distinct variables b_i and b_j. The partial derivative $\partial \mathbf{Y}/\partial b_i$ represents the sensitivity of $\mathbf{Y}$ with respect to b_i, and it is evaluated at the mean values of the b_i. Specifying the b_i to be mutually independent, the second term on the right-hand side of (4) vanishes. The variance of $\mathbf{Y}$ simplifies to

$$Var(\mathbf{Y}) = \sum_{i=1}^{n}\left(\frac{\partial \mathbf{Y}}{\partial b_i}\right)^2 Var(b_i) \tag{5}$$

When the second-order term in the Taylor expansion is incorporated, the mean of $\mathbf{Y}$ is refined by the second-order approximation

$$\bar{\mathbf{Y}} = \mathbf{Y}(\bar{b}_1, \bar{b}_2, \ldots, \bar{b}_n) + \frac{1}{2}\sum_{i=1}^{n}\left(\frac{\partial^2 \mathbf{Y}}{\partial b_i^2}\right)Var(b_i) \tag{6}$$

where the second derivatives are also evaluated at the mean values of the b_i. To estimate the second-order variance of $\mathbf{Y}$, the third and the fourth moments of the b_i are required, but those quantities are difficult, at best, to obtain. In the present simulations, the first-order variance of the response is generally sufficiently accurate for most practical problems, and for that reason, the variance and the mean of $\mathbf{Y}$ are calculated through (5) and (6).

When the variable b_i follows a specific probability distribution, its variance can be determined by its "tolerance," which is a more frequently-used term in manufacturing applications. The variance and tolerance are related by

$$Var(b_i) = \frac{1}{9}T_{b_i}^2 \tag{7}$$

for the normal distribution [15], and by

$$Var(\mathbf{b}_i) = \frac{1}{3}T_{b_i}^2 \tag{8}$$

for the uniform distribution [15], where T_{b_i} represents the tolerance of variable b_i. Once the tolerance of a design variable is known, the variance of the design variable can be calculated through (7) or (8). To calculate the statistical properties of $\mathbf{Y}$ from (5)-(6) along with (7)-(8) when the tolerance T_{b_i} is known, the first-order sensitivity $\partial \mathbf{Y}/\partial b_i$ and the second-order sensitivity $\partial^2 \mathbf{Y}/\partial b_i^2$ are required.

3. Sensitivity analysis of dynamic equilibria

In three-dimensional space, the configuration of a free rigid body is described by six coordinates, and the coordinate set of the i-th body in a multibody system is denoted here as $\mathbf{x}_i$. Quantities in bold typeface denote vectors or matrices. With the system comprising n rigid bodies, the system-level set of Cartesian coordinates

$$\mathbf{x} = \begin{bmatrix} \mathbf{x}_1^T & \mathbf{x}_2^T & \cdots & \mathbf{x}_n^T \end{bmatrix}^T \tag{9}$$

encompasses sets for the individual bodies. In the most general case, the equations of motion for a constrained multibody system can be expressed [20, 21]

$$\mathbf{M}\ddot{\mathbf{x}} + \boldsymbol{\Phi}_{\mathbf{x}}^T\boldsymbol{\lambda} = \mathbf{Q} \tag{10}$$

where $\mathbf{M}$, $\mathbf{Q}$, and $\boldsymbol{\lambda}$ denote the generalized mass matrix, the generalized force vector, and the Lagrange multiplier vector, respectively. The Jacobian constraint matrix $\boldsymbol{\Phi}_{\mathbf{x}}$ comprises partial derivatives of the constraint equations $\boldsymbol{\Phi}$ with respect to the set of coordinates in Eq. (9).

The equations of motion are cast in a reduced form by introducing the relative generalized coordinates $\mathbf{q}$ through

$$\dot{\mathbf{x}} = \mathbf{B}\dot{\mathbf{q}}, \tag{11}$$

where $\mathbf{B}$ is the velocity transformation matrix [9]. When the multibody system is in dynamic equilibrium, a subset of the $\dot{\mathbf{q}}$, denoted by $\dot{\mathbf{q}}_P$, defines the constrained system's constant rotational motions. The remaining $\dot{\mathbf{q}}$ are denoted by $\dot{\mathbf{q}}_R$. Eq. (11) then becomes

$$\dot{\mathbf{x}} = \mathbf{B}_P \dot{\mathbf{q}}_P + \mathbf{B}_R \dot{\mathbf{q}}_R \tag{12}$$

where $\mathbf{B}_P$ and $\mathbf{B}_R$ are the velocity transformation matrices associated with $\mathbf{q}_P$ and $\mathbf{q}_R$.

By using Eq. (12), the equations of motion (10) are reduced to [7]

$$\mathbf{M}^*\ddot{\mathbf{q}}_R + \boldsymbol{\Phi}_{\mathbf{q}_R}^{cT}\boldsymbol{\lambda}^c = \mathbf{Q}^* \tag{13}$$

where

$$\mathbf{M}^* = \mathbf{B}_R^T\mathbf{M}\mathbf{B}_R, \tag{14}$$

$$\mathbf{Q}^* = \mathbf{B}_R^T\mathbf{Q} - \mathbf{B}_R^T(\mathbf{M}\dot{\mathbf{B}}_P\dot{\mathbf{q}}_P + \mathbf{M}\dot{\mathbf{B}}_R\dot{\mathbf{q}}_R), \tag{15}$$

Note that $\ddot{\mathbf{q}}_P$ is zero vector since $\dot{\mathbf{q}}_P$ is constant. $\boldsymbol{\Phi}^c$ represents the cut-joint constraints at any points where kinematic chains in the system were cut to generate a tree structure [8]. A closed loop system contains one or more independent, but closed, kinematic loops, and it can be transformed into an open loop system by conceptually cutting internal joints. In that view, the number of cut joints is same as the number of closed loops. The acceleration constraint equations become

$$\boldsymbol{\Phi}_{\mathbf{q}_R}^c\ddot{\mathbf{q}}_R = \boldsymbol{\gamma}^c \tag{16}$$

where

$$\boldsymbol{\gamma}^c = -(\boldsymbol{\Phi}_{\mathbf{q}_R}^c\dot{\mathbf{q}}_R)_{\mathbf{q}_R}\dot{\mathbf{q}}_R - 2\boldsymbol{\Phi}_{\mathbf{q}_R t}^c\dot{\mathbf{q}}_R - \boldsymbol{\Phi}_{tt}^c \quad . \tag{17}$$

Eqs. (13) and (16) govern the dynamics of a constrained multibody system.

In a state of dynamic equilibrium, the $\mathbf{q}_R$ are constant. Therefore, $\dot{\mathbf{q}}_R$, $\ddot{\mathbf{q}}_R$, and $\ddot{\mathbf{q}}_P$ become zero at dynamic equilibrium state. At that condition, the roots of the following nonlinear homogeneous algebraic equations Π and Φ^c then determine the exact dynamic equilibrium positions and Lagrange multipliers:

$$\Pi(\mathbf{q}_R) = \mathbf{B}_R^T(\mathbf{M}\dot{\mathbf{B}}_P\dot{\mathbf{q}}_P - \mathbf{Q}) + \boldsymbol{\Phi}_{\mathbf{q}_R}^{cT}\boldsymbol{\lambda}^c = \mathbf{0} \tag{18}$$

$$\Phi^c(\mathbf{q}_R) = \mathbf{0}. \tag{19}$$

A Newton-Raphson algorithm [22] is used to find the solutions. However, the standard Newton-Raphson method breaks down at points where the Jacobian matrix is singular.

The sensitivity of the equilibrium configuration with respect to the scalar design variable b is considered next. By differentiating Eqs. (18) and (19) with respect to the design variable b, the sensitivity equations now become

$$\Pi_{\mathbf{q}_R}\mathbf{q}_R^b + \Pi_{\boldsymbol{\lambda}^c}\boldsymbol{\lambda}^{cb} + \Pi_b = \mathbf{0} \tag{20}$$

$$\Phi_{\mathbf{q}_R}^c\mathbf{q}_R^b + \Phi_b^c = \mathbf{0}. \tag{21}$$

In the final step, Eqs. (20) and (21) are written in the matrix form

$$\begin{bmatrix} \Pi_{\mathbf{q}_R} & \Phi_{\mathbf{q}_R}^{cT} \\ \Phi_{\mathbf{q}_R}^c & 0 \end{bmatrix}\begin{bmatrix} \mathbf{q}_R^b \\ \boldsymbol{\lambda}^{cb} \end{bmatrix} = \begin{bmatrix} -\Pi_b \\ -\Phi_b^c \end{bmatrix} \tag{22}$$

in terms of sensitivities for the coordinate vector $\mathbf{q}_R$ and the Lagrange multipliers $\boldsymbol{\lambda}^c$ at the dynamic equilibrium positions.

Since the Newton-Raphson method is used in calculating the dynamic equilibrium positions, the Jacobian matrix in Eq. (22) is the same as used in the Newton-Raphson iterations. Therefore, sensitivities of dynamic equilibria with respect to a design variable can be obtained by solving the linear Eqs. (22) after the calculation of the partial derivatives of the residual vector with respect to the design variable. The computational efficiency of the sensitivity analysis is facilitated by using the same Jacobian matrix, having already been calculated in the Newton-Raphson stage.

4. Applications and examples

In this section, two numerical examples are shown to demonstrate the performance of the present method. The first example is a spatially rotating double pendulum system, which evaluates its accuracy and computational efficiency for an open loop system. The second one is the mechanical speed governor mechanism, which verifies that the present method is applicable to a closed loop system. In particular, in the second example, various design parameters are considered. To verify the present method's accuracy, effectiveness, and computational efficiency, the calculated statistical results of examples are compared with those obtained from the traditional computationally-intensive Monte Carlo methods that were used previously.

4.1 Spatially rotating double pendulum

As the first example, Fig. 1 depicts a spatially-rotating 3-DOF (degree-of-freedom) double pendulum. This system consists of two single rigid bodies which form an open kinematic loop. The first uniform bar, illustratively of mass $m_1 = 3\ kg$ and length $L_1 = 1m$ is connected by a pin joint to a shaft that rotates about the vertical axis at a constant angular velocity Ω. The second uniform bar, illustratively of mass $m_2 = 3\ kg$ and length $L_2 = 1m$, is connected by a pin joint to the first bar. For a sufficiently high rotation rate, a stable equilibrium configuration with nontrivial θ_1 and θ_2 develops. With the generalized coordinate, constant at that condition, the scalar q_P and vector $\mathbf{q}_R$ become

$$\dot{q}_P = \Omega \tag{23}$$

$$\mathbf{q}_R = [\,\theta_1,\ \theta_2\,]^T . \tag{24}$$

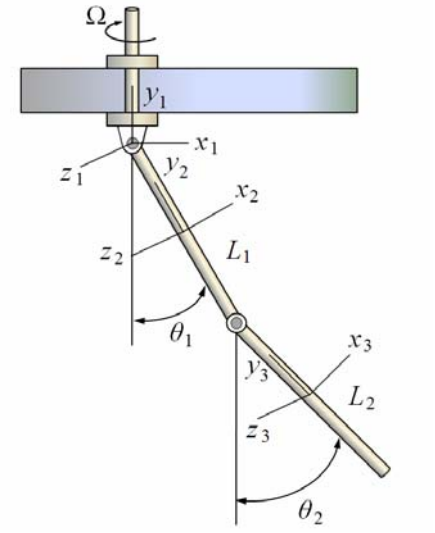

Fig. 1. A spatially-rotating double pendulum having nontrivial equilibrium positions at sufficiently high Ω.

Fig. 2 depicts the dependence of the system's equilibrium angles on the shaft's angular velocity. Only the trivial equilibrium is present for low shaft speeds, and that position bifurcates at the critical speed, which for the chosen parameter values becomes 2.67 rad/s. The trivial equilibrium bifurcates symmetrically with dynamic equilibria forming at both positive and negative values of θ_1 and θ_2. In what follows, the positive roots of Eq. (18) are taken.

The first bar's length, L_1, is taken as the design variable and the sensitivities of the dynamic equilibrium angles $\mathbf{q}_R$ with respect to L_1 can be obtained from Eq. (20).

Figs. 3 and 4 show the manner in which the standard deviations of dynamic equilibrium angles θ_1 and θ_2 depend upon the spindle's driving angular velocity. It is assumed in this study that the tolerance of L_1 has a normal distribution with 99.73% reliability. The variance of dynamic equilibrium angles can be obtained from Eqs. (5) and (7). The predictions of the present method are also compared with results from Monte Carlo simulation in Figs. 3 and 4; the two sets of results are nearly identical and barely distinguishable from one another on the scale of the figure. Table 1 compares performance of the Monte Carlo method with respect to the number of samples. However, the Monte Carlo approach requires some 30,000 simulation samples to achieve the same accuracy, and

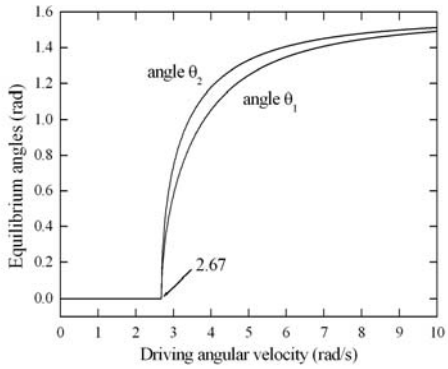

Fig. 2. Dynamic equilibrium positions (positive root) of a spatially-rotating double pendulum.

Table 1. Performance of the Monte Carlo method with respect to the number of samples. 0.3% of tolerance of the 1st link's length is considered.

Samples number	Error at 4.00 rad/s	Increase in computation time over the present method
1,000	3.35%	901%
5,000	1.64%	4,500%
30,000	0.22%	30,227%

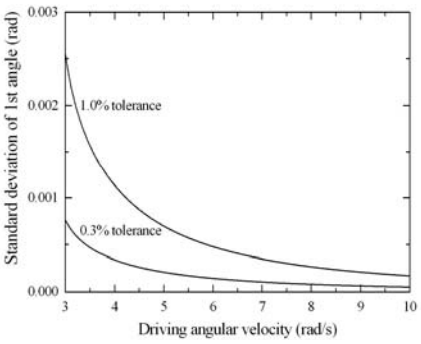

Fig. 3. Standard deviation of 1st angle with respect to the variation of the length of the 1st link. The present analytical solution (solid line) and the Monte Carlo simulation with 30,000 samples (dash-dot line) are nearly indistinguishable.

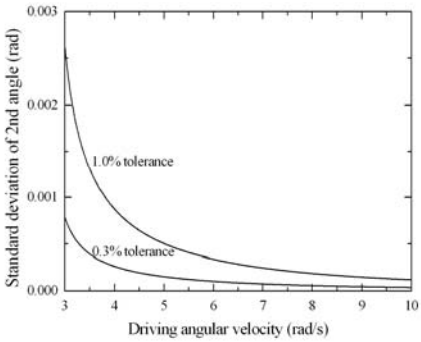

Fig. 4. Standard deviation of 2nd angle with respect to the variation of the length of the 1st link. The present analytical solution (solid line) and the Monte Carlo simulation with 30,000 samples (dash-dot line) are nearly indistinguishable.

a correspondingly high computational burden relative to the present approach.

Fig. 5 shows graphically the accuracy of the Monte Carlo method. As the number of samples of Monte Carlo simulation increases, the first angle's standard deviation line is close to the line which is obtained by the present analytical method. Therefore, the present method offers a substantial computational savings and accuracy that is independent of the sample size.

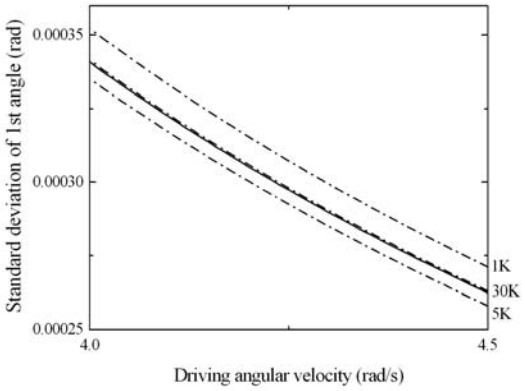

Fig. 5. Standard deviation of 1st angle. 0.3% of tolerance of the 1st link's length is considered. The solid line represents the present analytical solution and the dash-dot lines represent the Monte Carlo simulation results with respect to various samples (1,000, 5,000, and 30,000).

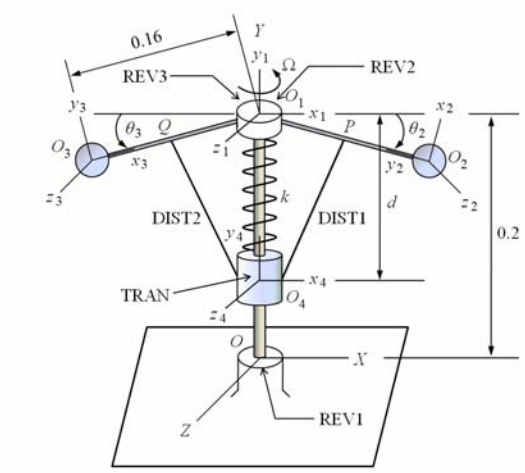

Fig. 6. A governor mechanism that has two closed kinematic loops, revolute joints labeled REV, a translational constraint TRAN, and the distance constraints DIST.

4.2 Mechanical speed governor mechanism

Fig. 6 shows a spatial 2-DOF governor mechanism formed of two closed kinematic loops. The first body is the upper spindle in which coordinate system $x_1 - y_1 - z_1$ is fixed and which is driven at angular velocity ω; the second and third bodies are pendulums having point masses at their outer ends; and the fourth body is the lower collar which is free to slide vertically on the spindle's axis. The spindle is connected to each pendulum through revolute joints, and the spindle and collar are connected by a translational joint and a spring k. Point O_i represents the center

Table 2. Inertia properties for rigid body elements that comprise the governor mechanism.

Body	Mass (kg)	*Ix'x'* (kg m^2)	*Iy'y'* (kg m^2)	*Iz'z'* (kg m^2)
Spindle	200	25	50	25
Mass 1	1	0.00036	0.00036	0.00036
Mass 2	1	0.00036	0.00036	0.00036
Collar	1	0.0004	0.00045	0.0004

Table 3. Initial coordinate values in global coordinates for the governor mechanism.

Point	X (m)	Y (m)	Z (m)
O_1	0	0.2	0
O_2	0.1131	0.0869	0
O_3	-0.1131	0.0869	0
O_4	0	0.05	0
P	0.0566	0.1434	0
Q	-0.0566	0.1434	0

of a body's Cartesian reference frame in space. For illustration, the collar and each pendulum are connected by joints having a fixed separation distance $0.1092\,m$, and the stiffness and the unstretched length of the spring are taken to be $1000\,N/m$ and $0.15\,m$. Table 2 lists the inertia properties of each component, and the coordinates of various points in Fig. 6 that define the system's configuration are listed in Table 3.

The constraint coordinate $\dot{q}_P$ is taken to be the driving angular velocity Ω, and the $\mathbf{q}_R$ are defined by

$$\mathbf{q}_R = [\, d, \theta_2, \theta_3 \,]^T, \tag{25}$$

where d is the relative translational distance between the spindle and the collar, and θ_2 and θ_3 are the relative angles of the revolute joints 2 and 3. In the system's initial state, the relative distance d is set at $0.15\,m$ and θ_2 and θ_3 are assigned at 0.7854 rad, respectively.

Fig. 7 shows the manner in which the dynamic equilibrium position, as measured by d, depends upon the spindle's driving angular velocity. The separation between the spindle and collar decreases monotonically with speed. The first design parameter of interest in this case is taken to be the spring's stiffness k, and the sensitivities with respect to k are obtained from Eq. (22). Fig. 8 depicts the manner in

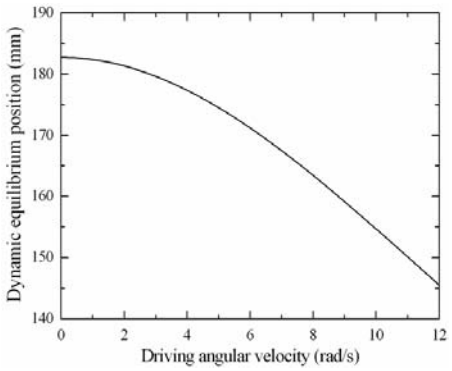

Fig. 7. Dynamic equilibrium position d of the governor's collar.

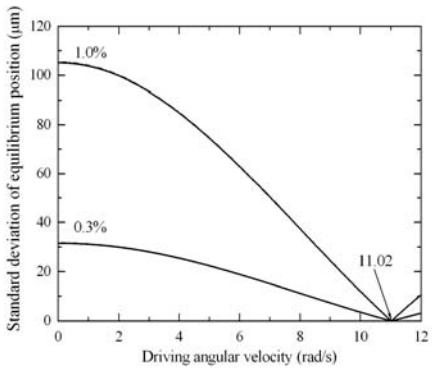

Fig. 8. Standard deviation of equilibrium position d with respect to the variation of the spring's stiffness. The present analytical solution (solid line) and the Monte Carlo simulation with 30,000 samples (dash-dot line) are nearly indistinguishable.

which the standard deviation of the collar's equilibrium position depends on the spindle's angular velocity. It is assumed in this study that the tolerance of a spring's stiffness has a normal distribution with 99.73% reliability. 0.3% and 1.0% of manufacturing tolerances are considered. The variance of dynamic equilibrium position can be obtained from Eqs. (5) and (7). The predictions of the present method are also compared with results from Monte Carlo simulation in Fig. 8; the two sets of results are nearly identical and barely distinguishable from one another on the scale of the figure.

In particular, when the spindle's driving angular velocity is set at $11.02\,rad/s$, the standard deviation of dynamic equilibrium position becomes zero. Therefore, the manufacturing tolerance and small variation in spring's stiffness have no effect on dynamic equilibrium position d at the $11.02\,rad/s$

operating point. The reason is that the dynamic equilibrium position becomes the same value of the unstretched length of the spring, and consequently the resultant spring force becomes zero when the spindle's angular velocity is set at $11.02\ rad/s$.

Table 4 compares the performance of the Monte Carlo method with respect to the number of samples. Fig. 9 shows graphically the accuracy of the Monte Carlo method. However, to achieve reliable statistical results from the Monte Carlo method requires some 30,000 simulation samples and a correspondingly high computational burden relative to the present method. Therefore, the present method offers a substantial computational savings and accuracy.

Fig. 10 shows a parametric study of the standard deviations of collar's equilibrium position. Three design parameters are considered: the spring's stiffness, ball's mass, and the distance joint's attachment points, the relative positions of points P and Q. Similarly, there are three zero standard deviation points, respectively. In this study, 0.3% of the tolerance for each design parameter is considered.

Table 4. Performance of the Monte Carlo method with respect to the number of samples. 0.3% of tolerance of spring's stiffness is considered.

Samples number	Error at 4.00 rad/s	Increase in computation time over the present method
1,000	3.40%	1,516%
5,000	1.63%	8,043%
30,000	0.22%	47,383%

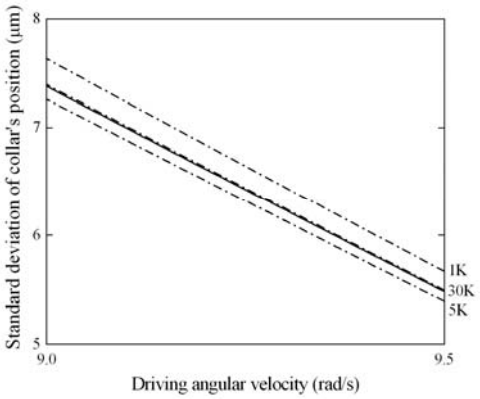

Fig. 9. Standard deviation of collar's equilibrium position. 0.3% of tolerance of spring's stiffness is considered. The solid line represents the present analytical solution and the dash-dot lines represent the Monte Carlo simulation results with respect to various samples (1,000, 5,000, and 30,000).

In order to verify the effectiveness of the zero standard deviation point, Monte Carlo simulations were conducted with increasing the tolerance value. The ball's mass was chosen as the design parameter, since it is relatively easier to adjust the mass than the spring's stiffness in the field of manufacturing. Table 5 further compares the standard deviations of the dynamic equilibrium position d at the zero standard deviation point 8.85 rad/s with those at the near 9.00 rad/s. 30,000 samples were used in those simulations. It is noticeable that the standard deviation of d at 8.85 rad/s with 30% tolerance value is much smaller than that at 9.00 rad/s with 0.3% tolerance value.

Therefore, these three zero standard deviation points are useful design points, because variation in each parameter's value has nearly no effect on dynamic equilibrium position d at each zero standard deviation point. The optimum design point which satisfies the maximum allowable manufacturing design spec can be also found from composing an optimization problem with three design parameters.

Table 5. Standard deviations of dynamic equilibrium position d with respect to the various tolerance values of ball's mass at the driving angular velocity 8.85 rad/s and 9.00 rad/s.

Tolerance (%)	Standard deviation of d at Ω = 8.85 *rad/s* (μm)	Standard deviation of d at Ω = 9.00 *rad/s* (μm)
0.03	0.000938	0.534
10	0.031	17.790
20	0.063	35.590
30	0.094	53.418

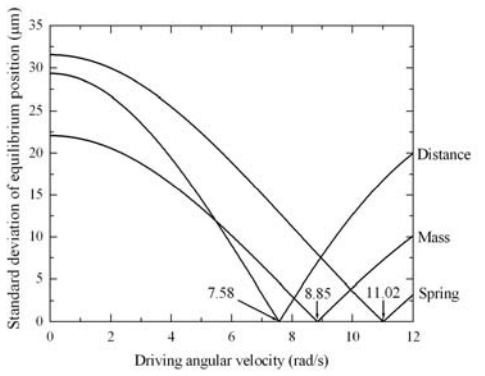

Fig. 10. Standard deviation of the collar's position with respect to 3% of tolerances of various parameters; spring's stiffness, ball's mass, and the attachment points of distance joint, P and Q. The present analytical solution (solid line) and the Monte Carlo simulation with 30,000 samples (dash-dot line) are nearly indistinguishable.

5. Conclusions

This paper presents a statistical approach for the effects of manufacturing tolerances on dynamic equilibria of a spatial multibody system undergoing prescribed rotational motion. In this work, the tolerances of various design parameters including lengths, stiffnesses, inertias, and attachment positions are examined. In order to analytically calculate the statistical response of the dynamic equilibria to such tolerances, the first-order and the second-order of sensitivity information of dynamic equilibrium positions with respect to the design parameter are necessitated. Therefore, a new numerical algorithm for calculating the first-order sensitivities of dynamic equilibria based on the direct differentiation method is derived and the second-order sensitivities can be obtained by numerical procedures using finite differences. A general multibody formulation, relative coordinates, and a velocity transformation technique are used to obtain the equations of motion and to identify the dynamic equilibria. In order to verify the present method's accuracy and computational efficiency, two numerical examples are described: an open loop and a closed loop system. The standard deviations obtained analytically are compared with those obtained by Monte Carlo simulations with various sample numbers. However, in order to obtain reasonable results, the Monte Carlo method requires a huge number of samples and very expensive computational cost. The present analytical method offers substantial improvement in computational efficiency when compared to the traditional Monte Carlo method. In some cases, an interesting equilibrium configuration having an operating condition for which the response has zero standard deviation to perturbations of a design parameter was found. That condition can be a useful design point to the extent that typical manufacturing tolerances or other sources of variation would have no effect on the dynamic equilibrium configuration.

Acknowledgments

This work was supported in part by the Korean Government and the Korea Research Foundation (MOEHRD) under grant KRF-2006-352-D00005.

References

[1] A. A. Shabana, Dynamics of Multibody Systems, second ed., Cambridge University Press, Cambridge, (1998).

[2] J. H. Ginsberg, Mechanical and Structural Vibrations, Theory and Applications, John Wiley & Sons, Inc., New York, (2001).

[3] T. R. Kane and D. A. Levinson, Dynamics: Theory and Applications, McGraw-Hill, New York, (1985).

[4] MSC Software Inc., ADAMS 2005 r2 User's Guide, (2005).

[5] FunctionBay Inc., RecurDyn v6.2 User's Guide, (2006).

[6] INTEC, SIMPACK User's Guide, (2006).

[7] D. H. Choi, J. H. Park and H. H. Yoo, Modal analysis of constrained multibody systems undergoing rotational motion, *Journal of Sound and Vibration* 280 (1) (2005) 63-76.

[8] D. S. Bae and E. J. Haug, A recursive formulation for constrained mechanical system dynamics: Part I. Open loop systems, *Mechanics of Structures and Machines* 15 (3) (1987) 359-382.

[9] S. S. Kim and M. J. Vanderploeg, A general and efficient method for dynamic analysis of mechanical systems using velocity transformations, *ASME Journal of Mechanisms*, *Transmissions and Automation in Design* 108 (2) (1986) 176-182.

[10] R. S. Hartenberg and J. Denavit, Kinematic Synthesis of Linkages, McGraw-Hill, New York, (1964).

[11] R. E. Garret and A. S. Hall, Effects of tolerance and clearance in linkage design, *ASME Journal of Engineering for Industry* 91 (1969) 198-202.

[12] S. Dobowsky and F. Freudenstein, Dynamic analysis of mechanical systems with clearances, Part 1: Formulation of dynamic model, *ASME Journal of Engineering for Industry* 90 (1971) 305-316.

[13] P. A. Ravn, Continuous analysis method for planar multibody systems with clearance, *Multibody System Dynamics* 2 (1) (1988) 1-24.

[14] P. Flores, J. Ambrosio and J. C. P. Claro, H.M. Lankarani, Dynamics of multibody systems with spherical clearance joints, *ASME Journal of Computational and Nonlinear Dynamics* 1 (3) (2006) 240-247.

[15] S. J. Lee, Performance Reliability and Tolerance Allocation of Stochastically Defined Mechanical Systems. Ph.D. Dissertation, Pennsylvania State University, (1989).

[16] S. J. Lee and B. J. Gilmore, The determination of the probabilistic properties of velocities and accelerations in kinematic chains with uncertainty,

ASME Journal of Mechanical Design 113 (3) (1991) 84-90.

[17] K. W. Chase, J. Gao and S. P. Magleby, General 2-D tolerance analysis of mechanical assemblies with small kinematic adjustments, *Journal of Design and Manufacture* 5 (1985) 263-274.

[18] D. H. Choi, S. J. Lee and H. H. Yoo, Dynamic analysis of multi-body systems considering probabilistic properties, *Journal of Mechanical Science and Technology* 19 (2005) 133-139.

[19] W. Schiehlen, N. Guse and R. Seifried, Multibody dynamics in computational mechanics and engineering applications, *Computer Methods in Applied Mechanics and Engineering* 195 (2006) 5509-5522.

[20] P. E. Nikravesh, Computer-Aided Analysis of Mechanical Systems, Prentice-Hall, Englewood Cliffs, New Jersey, (1988).

[21] E. J. Haug, Computer-Aided Kinematics and Dynamics of Mechanical Systems, Volume I: Basic Methods, Allyn and Bacon, Massachusetts, (1989).

[22] K. E. Atkinson, An Introduction to Numerical Analysis, Wiley, New York, (1978).